Proc. Schl. Eng. Tokai Univ., Ser. E
40 (2015) 89-96

A Study on Ostia Variation for Airflow Patterns within Nasal Cavity Models with Maxillary Sinus

by

Erny AFIZA[*1], Yoko TAKAKURA[*2], Taku ATSUMI[*3] and Masahiro IIDA[*4]

(Received on Mar. 31, 2015 and accepted on Jul. 9, 2015)

Abstract

In this study, airflow is numerically simulated within real models of the human nasal cavity to elucidate the effects of ostia features for ventilation of the maxillary sinus. Models of ostia are generated according to variation on number, position, and diameter for systematic investigation. Consequently, as for flow patterns within the main nasal cavity, almost no significant difference can be observed with or without the sinus in spite of a variation of diameter in the range of 2mm to 3mm. Regarding flows in the sinus with ostia variation, the following have been obtained: (1) Flow patterns change with variation of number and location of ostia, but not with variation of ostia diameter. (2) During the inhalation process, all models show the same tendency on the time history of mass flux entering the sinus as that given at the inlet boundary. During the exhalation process, in the standard model with an anterior ostium only, mass flux is negligible, while in the model with posterior ostium only, mass flux takes an inconsistent tendency with that at the inlet. The mass flux can be increased with the presence of multiple ostia. (3) Bigger ostia in diameter cause an increment in the mass flow rate but slight reduction in the mass flux entering the sinus due to the reduction of its velocity.

Keywords: Maxillary sinus, Ostia variation, Modelling, Numerical simulation, Unsteady flow

1. Introduction

Paranasal sinuses are paired air-filled spaces, and the certain reason for their existence, in fact, remains unclear except for reduction of weight in skull. As shown in Fig. 1, the maxillary sinus is the largest among four groups for human paranasal sinuses. It is generally stated that the presence of maxillary sinus can be related to humidification of the inhaled air, voice enhancement, and also as shock absorber in trauma. The pyramid-shaped space with averaged capacity of 10-15ml are located below the cheeks, above the teeth and on the side of nasal cavity lined by mucosal membrane. The shape, size and location of maxillary sinuses vary significantly not only between individuals, but also between each sides of the same person. They are connected to media meatus through single or multiple opening called ostium/ostia. These openings (ostia) are situated near the top of the maxillary sinus, which may cause difficulties in draining its contents to the nasal cavity by gravity. On the side of the main nasal cavity, the ostia are located mostly in the anterior/middle region of the middle meatus.

In general, human possesses only one ostium called natural ostium (NO) located around the media meatus. Having more than one ostium is thought to be a result of diseases such as rhinosinusitis and chronic maxillary sinusitis which can be related with the mucus circulation within these ostia [1, 2]. The existence other than NO is known as accessory ostia (AO). The population who have AO is said between 4% and 50%[3]. It is stated that cadaver models possess higher rates of having more than one ostium compared to in vivo models [3, 4]. The reason might be that the mucosal tissue shrinkage during the measurement process makes the ostium more apparent.

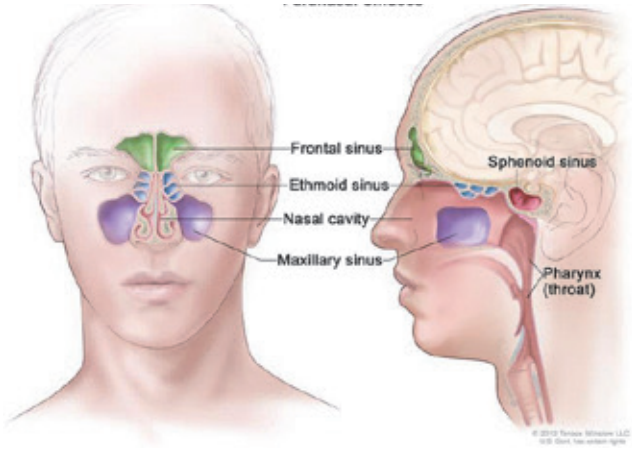

Fig. 1 Paranasal sinuses [5]

*1 Graduate Student, Course of Science and Technology
*2 Professor, Course of Science and Technology
*3 Assistant Professor, School of Medicine
*4 Professor, School of Medicine

R Aust, et al. has established a method for measuring the functional size of ostia in vivo on the basis of pressure rise[6]. It is stated that, the average of the ostia diameters was 2.4mm among 37 subjects and there is almost no significant difference in the volume of the maxillary sinus and the diameter of the ostium between men and women. Ho-yeol Jang, et al. performed a study regarding the changes in ostia diameter as a consequence from elevating the sinus floor through surgery[7]. Their findings showed that the diameters of ostia are significantly decreased with the elevation of the sinus floor, which caused sinus obstructions.

Obstruction in sinus causes reduction in sinus ventilation and drainage, which can increase the possibilities of having maxillary sinus-related diseases such as sinusitis, for example, clogging of the ostia, septal deviation, swelling of the membrane tissue and many more[8]. Up until now, surgical operation in sinusitis is in attempt to increase the ventilation of the sinus. If accurate information related to the variation of the ostia is obtained on the airflow pattern in real model of the nasal cavity including the human maxillary, it can greatly contribute the medical treatment.

In vivo experiment is regarded to be most actual in visualizing the airflow pattern. However, direct measurements in the human nasal cavity are almost impossible due to the complexity of the geometry: crooked bends and narrowness. For example, as an intrusive method, the capability of direct visualization technique such as hot wire anemometry is restrained considering the obstruction effect to the airflow itself and the biological reaction against physical contact[9]. On the contrary, numerical simulation is advantageous intreating complex geometry.

While there are many papers about flows within main nasal cavities, researches on ventilation of sinuses are very few. C. M. Hood, et al. investigated the gas exchange in human maxillary sinus on the variation of the ostia length and diameter numerically by using very simple geometries and confirmed that the presence of multiple ostia causes a rise in mass flow rate followed by ventilation rate increment[10]. In another study by J. H. Zhu et al, using models with real geometries, ventilation increment followed by increasing of the AO number is reported to be complicated. With the presence of more than one AO, the maximum mass flow rates through the maxillary sinus remains unchanged despite the changes in nasal airflow condition (high and low). Furthermore, a small transient airflow reversal was observed at the beginning and end of respiratory phases[11].

Features of ostia are important in discussing ventilation process of sinuses, but they vary between individuals as well as geometries of nasal cavities and sinuses. The fact makes the ventilation problem complicated. From this viewpoint, the authors made modelling for ostia features, but still keeping real geometries for the nasal cavity and maxillary sinus. Thus in ref. 12 a systematic investigation by CFD was carried out with modelling variation on number and position of ostia, and mass flow rates entering the sinus from the nasal cavity were compared among ostia models. A result is that the sinus ventilation can be increased with the presence of multiple ostia.

In this paper, the extensive study is shown with modelling variation further including ostia diameter in addition to number and position of ostia. In order to elucidate the effects of ostia features for the sinus ventilation, airflows are numerically simulated within real-geometric model of a human nasal cavity and maxillary sinus with systematic modelling of ostia features.

Table 1 : Variation of Models

Model	Ostia Features	Diameter of Ostia	Anterior Ostium	Posterior Ostium
A	Without sinus	-	-	-
B	Both Ostia	2 mm	exist	exist
C	Anterior only	2 mm	exist	-
D	Posterior only	2 mm	-	exist
E	Both Ostia	3 mm	exist	exist
F	Anterior only	3 mm	exist	-
G	Posterior only	3 mm	-	exist

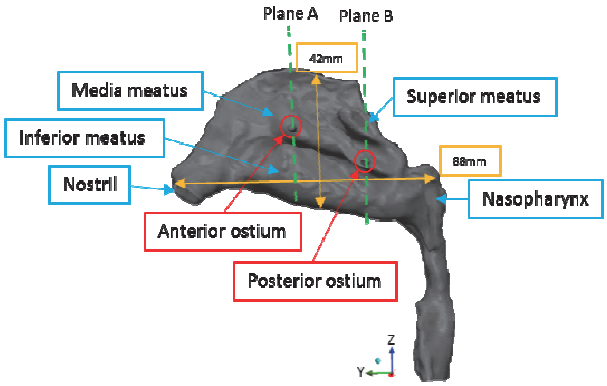

(a) Nasal cavity (Without maxillary sinus)

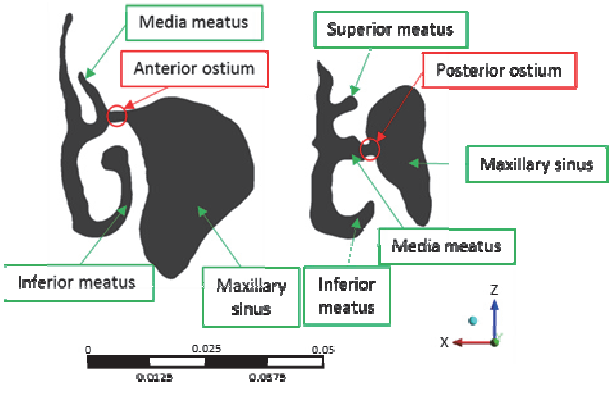

(b) Cross sectional section at Plane A (left) and B (right)

Fig. 2 Structure of Nasal Cavity with Maxillary Sinus

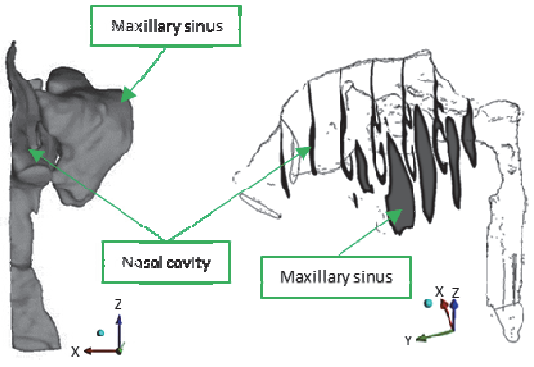

Fig. 3 Nasal Cavity with Maxillary Sinus (front and isometric view)

Fig. 4 Respiration cycle in regard to mass flux at nasopharynx area.

2. Computational method

2.1 *Generation of Models and Grids*

By collaboration with Tokai University Hospital, a highly detailed configuration model of the human nasal cavity was fabricated as shown in Fig. 2 and 3. The three-dimensional nasal cavity model was reconstructed from a Computer Tomographic scan (CT scan) with spatial resolution 512x512 pixels, obtained by 0.3mm slice width. Only one of the two nasal cavities was studied considering that the anatomy of the nasal cavities is almost identical.

A few features were disregard in this model: (a) nostril hairs, (b) external nose shape, and (c) properties of nasal tissues such as, moist and warm condition within the nasal cavity. The data was then imported into 3D slicer (The Slicer Community) for volume rendering. It is a free source software and has been widely used particularly in medical purposes. Next, software 3Ds Max Design (Autodesk inc.) was used to modify the 3D model of nasal cavity which includes deleting the unwanted features such as tongue, ethmoid sinuses, frontal sinus and many more. Feature variations with regard to the number and diameter of ostia, and smoothing process were also performed by using the same software [13]. The modified model was imported to ICEM CFD (ANSYS, inc.) by using STL data to generate the mesh consisting tetra elements in the inner region and 5 layers of prism elements near the wall before the airflow pattern was simulated by FLUENT 14.5 (ANSYS, Inc.). Seven types of human nasal cavity models with and without the presence of maxillary sinus on the variation of number and diameter of ostia (volume: 20.6ml) were created as shown in Table 1.

The anterior ostium is located in the anterior/middle side of middle meatus about 42mm in Y direction from nostril (See Fig. 2(a) about Y direction). Meanwhile, the posterior ostium is in the vicinity of the posterior side of middle meatus (65mm from nostril in Y direction). Model F is regarded to be the standard model with the presence of anterior ostium only which appears in more than half of healthy person[10]. As mean diameter of ostia for healthy persons is about 2.4mm, here 2mm and 3mm are adopted.

2.2 *Computational Condition*

Reynolds number of airflow is 880, which is obtained from the average hydraulic diameter of nares of the model at maximum breathing rate[14]. Airflows for incompressible fluid are computed using FLUENT under the following boundary conditions: (1) The nasal wall is rigid with non-slip condition; (2) A pressure of zero (Gauge pressure) is presumed at the nostril; (3) To mimic a natural breathing airflow, user defined function is utilized to simulate unsteady condition where the maximum flow velocity of 1.9m/s is given at the nasopharynx area. In real life of human respiration, the inhalation process takes slightly more time compared to expiration process [15]. However, in reference from a few studies, human respiration cycle is represented by sinusoidal curve of flow rate imposed at the nasopharynx area [16, 17], and in this investigation the similar respiration model is used. Periodic cycles for breathing start with the steady-state flow solution at maximum inhalation and followed by exhalation, with period time of 3 seconds in each cycle. Simulation was performed for 3 cycles (9000 time-steps), achieving a converged solution at each time-step. The third cycle was evaluated as solution during one period. In mass flux at the inlet (nasopharynx side) in responds to the time as shown in Fig. 4, 6 and 7.5 seconds represent the peak inhale and peak exhale, respectively.

2.3 *Grid Convergence*

In order to obtain more accurate results, before moving onto the simulation, calculation on the grid convergence was performed where the mesh is refined until the solution for the specified variable is converged to values independent on mesh size. By changing the global element factor of ICEM CFD, in Model E, five types of grids with different mesh size were generated with 1 million cells being the coarsest and 5.8 million cells being the finest. Mesh in the ostia regions was set to the ratio of 90% smaller than the global element size in all types of grids to ensure more detailed results in the particular area.

For the steady solution of inspiration the pressure values at a point defined near the nasopharynx area are compared among all grids. As shown in Fig. 5(a), the grid resolution was converged as the grid approached 5.8 million cells with only 0.3% pressure difference with grid of 5 million cells. To save computing time and memory, the grid with 5 million cells was chosen to be the standard one throughout the present study. As illustrated in Fig. 5(b), for models with 2mm ostia, model with 2.1 million cells was used[12].

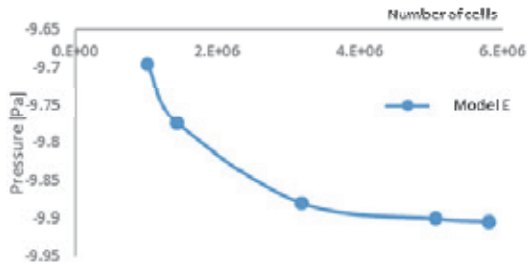

(a) Model E (3mm ostia)

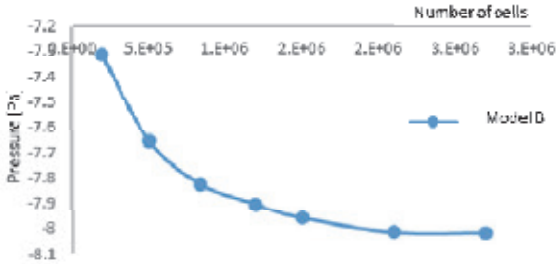

(b) Model B (2mm ostia)

Fig. 5 Grid convergence in respect to pressure at nasopharynx area

3. Computational results

The airflow patterns are shown by instantaneous streamlines. For flow patterns within the sinus, streamlines passing through the plane placed at the middle of ostia are drawn. Meanwhile, velocity vectors within ostia are drawn as projection on the plane.

3.1 *Without Maxillary Sinus*

Numerical results in model of the nasal cavity without maxillary sinus are presented in instantaneous streamlines at peak inspiration and expiration in Fig. 6. During inspiration, the highest velocity distribution in the nasal cavity was recorded along the media meatus. A fairly large swirl was detected near the olfactory region in the superior meatus. Moreover, reversed-like flow was also found in the inferior meatus before entering the nasopharynx.

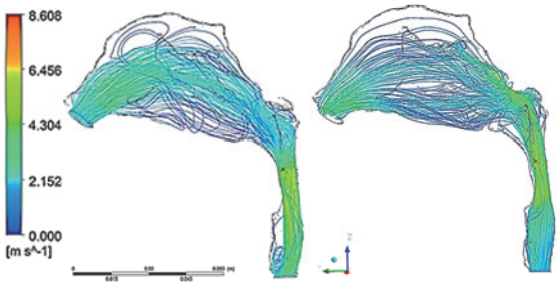

(a) Inspiration (b) Expiration

Fig.6 Instantaneous streamlines in nasal cavity of Model A

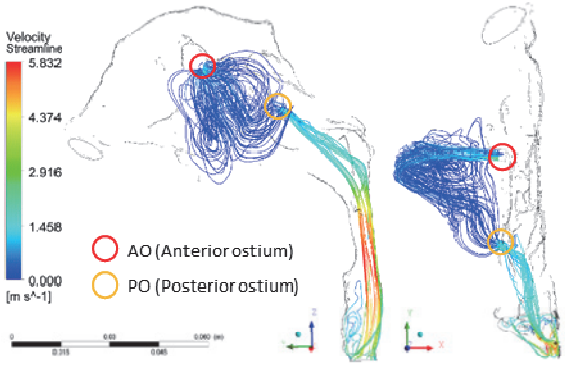

(a) Peak inspiration

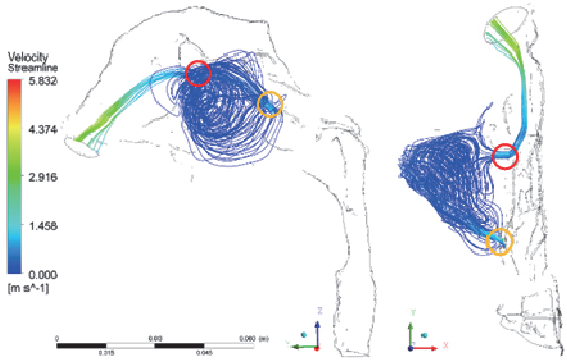

(b) Peak expiration

Fig. 7 Instantaneous streamlines in sinus of Model E (side and top view)

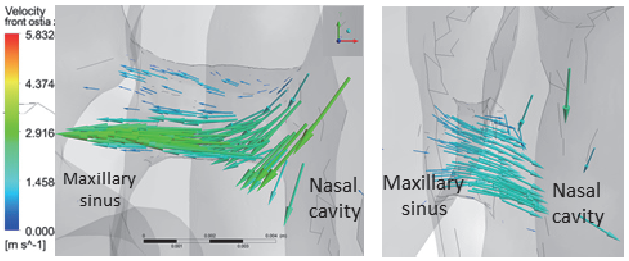

(a) Peak inspiration

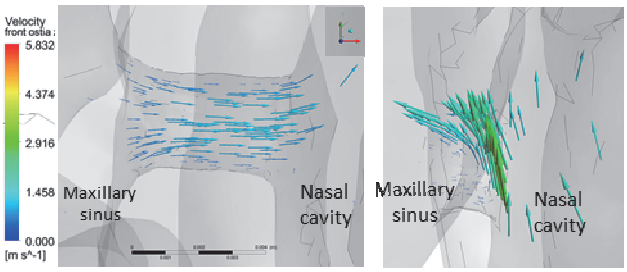

(b) Peak expiration

Fig. 8 Velocity vectors in anterior (left) and posterior (right) ostia

Meanwhile during expiration, the mainstream is located along media and inferior meatus. A small-scale swirl was observed at the inferior meatus at the posterior side of the cavity.

Almost no discrepancy can be observed in airflow patterns within the main nasal cavity between Model A and models with maxillary sinus (Models B, C, D, E, F and G) despite the changes in the ostia diameter.

3.2 *Presence of both anterior and posterior ostia (3mm)*

Instantaneous streamlines within the sinus in Model E (with both ostia) at peak inspiration and expiration is shown in Fig. 7, where the red and yellow circle represents AO and PO, respectively. In general, the flow is distributed in all region of the sinus during both cases of inspiration and expiration. However, discrepancy on the pattern can be observed, as the flow can be seen divided into two during inspiration, and otherwise during expiration.

Fig. 8(a) shows the velocity vectors in anterior and posterior ostia at peak inspiration. During inspiration, generally, the flow is introduced to the sinus through the anterior ostium, and exits at the posterior ostium. Meanwhile during expiration in Fig. 8(b), the flow enters the sinus through the posterior ostium and exits at the anterior ostium. A small vorticity occurs at the posterior ostium in the side of maxillary sinus.

3.3 *Presence of anterior ostium only (3mm)*

With the presence of anterior ostium only, in Model F at peak inspiration, in Fig. 9(a), so many streamlines cannot be detected for the same velocity magnitude as in Model E. In view of velocity vectors in Fig. 10(a), the airflow generates a vortex with fairly high velocity at the ostium area, with nearly half of its velocity vectors going toward the sinus and the other half returning to the nasal cavity even before entering the sinus. Meanwhile during expiration, a flow circulates at the entrance

of the anterior ostia with very small tendency of going into the sinus (Fig. 10(b)), so that streamlines cannot be detected in Fig. 9(b).

3.4 *Presence of Posterior ostium only (3mm)*

From Figs. 11(a) and (b), although the flow circulation area detected in Model G is larger compared to Model F, it is smaller than in Model E. As shown in Figs. 12(a) and (b), during inspiration and expiration, a vortex can be observed at the ostium as the flow tends to flow into and out of the sinus. Similar to previous results, the swirl takes charge of the inflow and outflow of the ostia.

3.5 *Mass flux*

In Fig. 13, 14 and 15 for the mass flux or mass flow rate entering the sinus through ostia, the cases of both ostia (Models B and E) indicate the inflow through the anterior ostium).

Figure 13 shows the time history of mass flux entering the 3mm ostia.In Model E, the mass flux entering the sinus is at its maximum in corresponding to the peak mass flux at inlet in the nasal cavity model in Fig. 4. However, during expiration, no obvious peak can be observed.

For models with one ostium only (Model F and G), the entering mass flux is much lower in comparison to that in model with both ostia (Model E). In the standard model (Model F), the entering mass flux takes its maximum at peak inhalation, while it remains little during expiration process. With the presence of posterior ostium only in Model G, the entering mass flux is almost the same compared to Model F during inspiration, but noticeably higher during expiration.

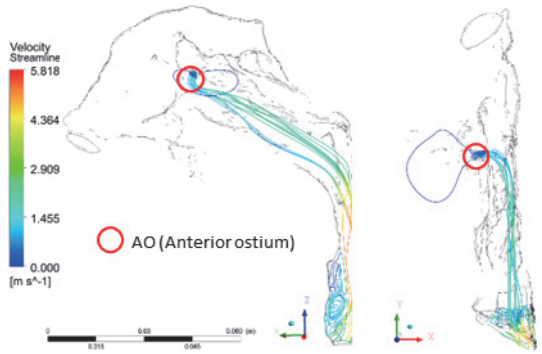

(a) Peak inspiration

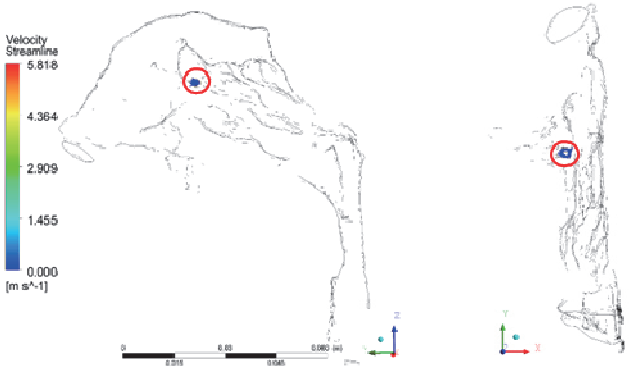

(b) Peak expiration

Fig. 9 Instantaneous streamlines in sinus of Model F (side and top view)

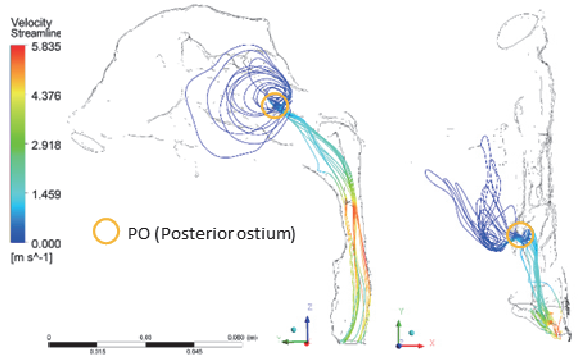

(a) Peak Inspiration

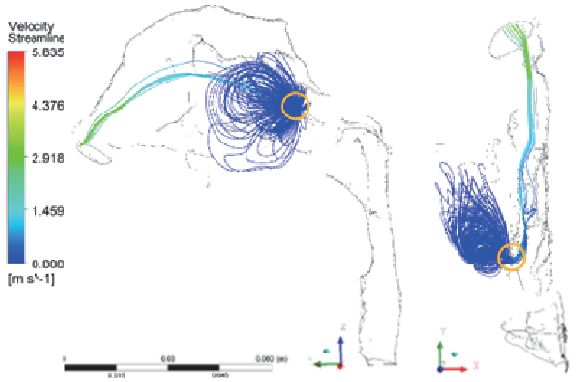

(b) Peak Expiration

Fig. 11 Instantaneous streamlines in sinus in Model G (Side and Top view)

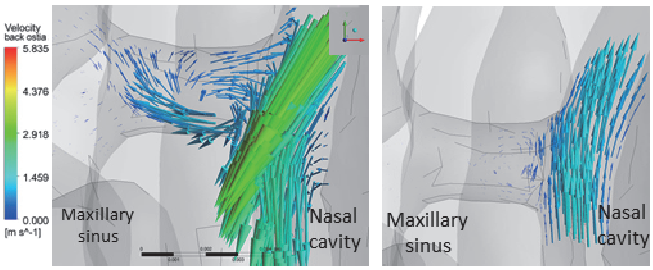

(a) Peak inspiration (b) Peak expiration

Fig. 10 Velocity vectors in anterior ostium only

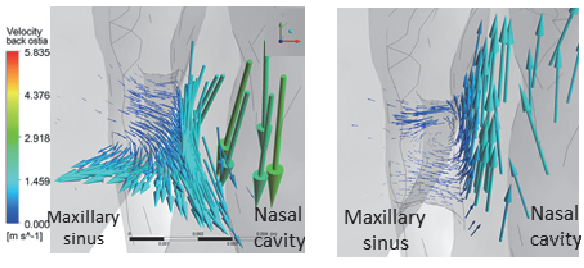

(b) Peak inspiration (b) Peak expiration

Fig. 12 Velocity vectors in posterior ostium only

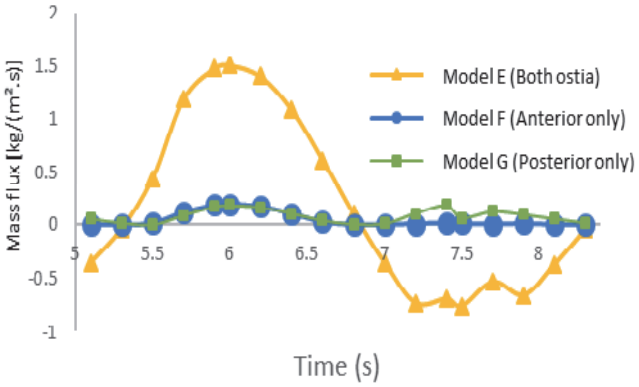

Fig. 13 Mass flux entering sinus through 3mm ostia

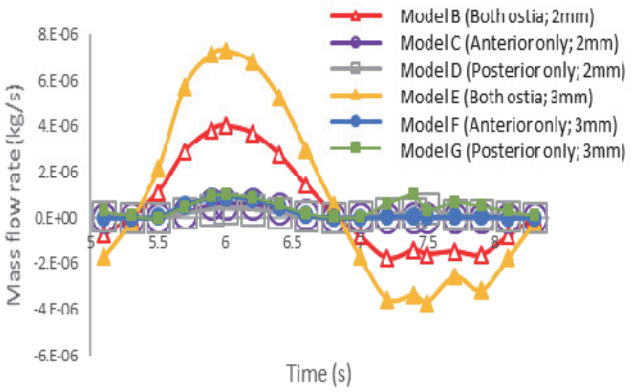

Fig. 14 Mass flow rate entering sinus through ostia

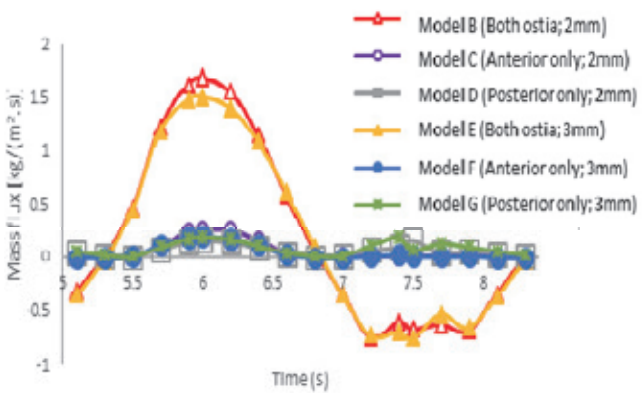

Fig. 15 Mass flux entering sinus through ostia

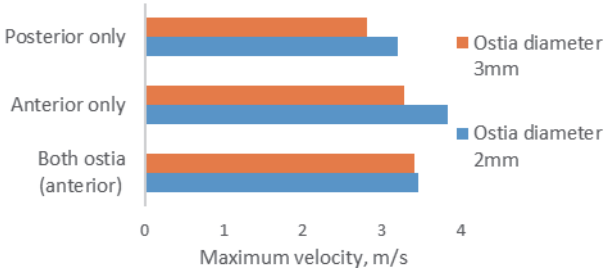

Fig. 16 Maximum velocity in ostia at peak inhalation

3.6 *Comparison between 2mm and 3mm ostia*

As for the comparison between 2mm and 3mm ostia, almost no significant difference can be observed in the airflow pattern in both streamlines in the maxillary sinus and velocity vectors in the ostia for all cases. Meanwhile, regarding the mass flow rate results (Fig. 14), the ventilation of sinus increases in models with 3mm ostia compared to that in models with 2mm ostia. However, in the mass flux results (Fig. 15), the mass flux entering the 2mm ostia is slightly higher than 3mm ostia in most cases (models with both ostia and anterior ostium only). Fig. 16 illustrates that the maximum velocity at peak inhalation is higher in the 2mm ostia compared to the 3mm ostia in all cases. The bigger ostia causes a reduction in its velocity, and thus lowers the mass flux entering the maxillary sinus during inspiration.

4. Discussions

Regarding the distribution of streamlines, with the presence of both ostia in Model E, the flow distributes in all region within the sinus during inspiration and expiration, on the contrary to the models with the existence of one ostium only.

With the presence of two ostia (anterior and posterior) in Model E, the mass flux value is much bigger than that in the models with one ostium only (anterior or posterior) as the flow enters and exits at different ostia. Meanwhile, with the existence of single ostium (anterior or posterior), a swirl appears in the ostium, which is in charge of flows into and out of the sinus at the same time. In Models E and F, the entering mass flux at the entrance of the sinus (i.e., at the ostium) during peak inhalation is higher compared to that during exhalation. On the other hand, in Model G, the entering mass flux is almost same at peak inhalation and exhalation.

In view of the standard model (Model F with anterior ostium only), ventilation is much smaller in comparison to that in the Model E. This phenomenon might help to prevent the mucosal surface of the maxillary sinus from drying and to maintain high nitric oxide concentration in the sinus itself[18]. High nitric oxide concentration within the sinus can be related in preventing pathogen from spreading in the sinus [8, 19]. Moreover, the entering mass flow rate is higher during inhalation, which might be related to its function, to warm and humidify the inhaled air. Extensive studies on the effect of ostia variation on this matter might give insights in its relevancy to the nasal cavity physiology.

To investigate the reliability of the present ostia models, the present results with two ostia of 3mm are compared with study with J. H. Zhu [20], where numerical simulations were carried out to assess the airflow ventilation in nasal cavity, maxillary sinus, and two ostia before and after surgery in three cases with different nasal ventilation rate: calm breathing, light breathing, and heavy breathing. Results in calm breathing was chosen to be compared with current study. Figure 17 illustrates the comparison on the sinus ventilation between both results. Both results show the similar tendency that the air entering the sinus has the maximum value at peak inspiration, while it is irregular during exhaling. In Zhu's study, the size of NO is almost the same but the size of AO is smaller in comparison to the current study, which might cause the discrepancy in magnitude of the sinus ventilation during expiration.

Thus, it has been confirmed that the present ostia models are effective to comprehend the complicated flow phenomena about the sinus ventilation.

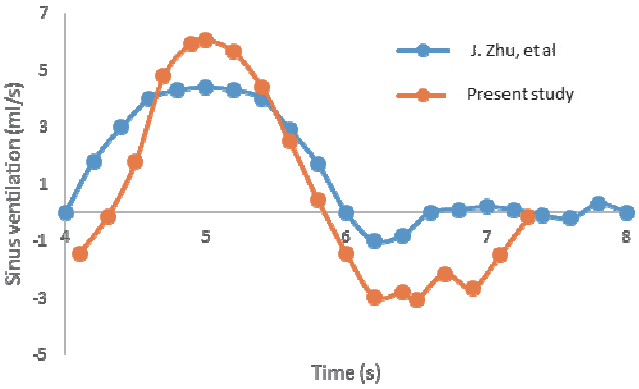

Fig. 17 Comparison in sinus ventilation between present study and J. Zhu et al.

5. Conclusions

In this research, models of the maxillary sinus with variation of number, position, and diameter of ostia were attached to the middle meatus of the main nasal cavity.

As for flow patterns of within the main nasal cavity, almost no significant difference can be observed with or without the maxillary sinus in spite of variation of diameter in the range from 2mm to 3mm.

Regarding flows in the sinus with ostia variation, the followings have been obtained:

(1) Flow pattern within the maxillary sinus:
Flow patterns change with variation of number and location of ostia, but do not with variation of ostia diameter;

(2) Mass flux entering the sinus:
During inhalation process, all models show the same tendency on the time history of mass flux as given at the inlet boundary. During exhalation process, in the standard model with an anterior ostium only, the mass flux is negligible, while in the model with a posterior ostium only, mass flux takes inconsistent tendency with that at the inlet. The mass flux can be increased with the presence of multiple ostia as the flow enters and exits at different ostia;

(3) Mass flow rate and mass flux:
Bigger ostia in diameter causes an increment in the mass flow rate but slight reduction in the mass flux entering the sinus due to the reduction of its velocity.

Finally it has been confirmed that the present ostia models are effective to comprehend the complicated flow phenomena about the sinus ventilation.

Reference

1) Kane, K.: Recirculation of Mucus as a cause of Persistent Sinusitis. *American Journal of Rhinology and Allergy*, 11:270-272, 1997.

2) Matthews, B.L., Burke, A.J.: Recirculation of mucus via accessory ostia causing chronic maxillary sinus diseases. *Otolaryngology - Head and Neck surgery*, 117: 422-423, 1997.

3) Jog M, McGarry GW.: How frequent are accessory sinus ostia? *J Laryngol Otol* 117, 270-272, 2003.

4) Simon E.: Anatomy of the opening of the maxillary sinus *Arch Otolaryngol* 29, 640-649, 1939.

5) Aust, R., Drettner, B.,: The functional size of the human maxillary ostium in vivo. *Acta Otolaryngology* 78, 432-435, 1974.

6) http://www.cancer.gov/types/head-and-neck/patient/paranasal-sinus-treatment-pdq

7) Ho-yeol J., Seung-gul S., Jae-bong P., Hyoun-chull Kim., Il-hae P., Sang-chull L., The change of maxillary sinus ostium in diameter following sinus floor elevation surgery using cone beam computered tomography.W.-K. Chen, *Linear Networks and Systems*, Belmont, CA: Wadsworth, 123-135, 1993.

8) C. M. Hood, R. C. Schroter, D. J. Doorly, E. J. S. M. Blenke, N. S. Tolley: Computational modelling of flow and gas exchange in models of the human maxillary sinus, *J Appl Phsyiol*, 107:1195-1203, 2009.

9) D.I. Hahn, P.W. Scherer, and M.M. Mozell, Velocity Profiles Measured for Air-flow through a Large Scale Model of the Human Nasal Cavity, *J Appl Physiol*, 75: 2273-2287, 1993.

10) Proctor DF, Andersen I., The nose: upperway physiology and the atmospheric Environment, Amsterdam. *Elseveir Biomedical*, 1982.

11) J. H. Zhu, H. P. lee, K.M. Lim, B. R. Gordon, D. Y. Wang, Effect of accessory ostia on maxillary sinus ventilation: A computational fluid dynamics (CFD) study, *Respiratory Physiology and Neurobiology*, 183, 91-99, 2012.

12) E.Afiza, Y.Takakura, Y. Takakura, T. Atsumi, M. Iida: Effects of ostia variation for Airflow Patterns within Nasal cavity Models with Maxillary Sinus. *Journal of Medical and Bioengineering,* 2015.

13) M. Kajiyama and Y. Takakura (Supervisor), generation of nasal geometry models for fluid simulation from CT scan data, Bachelor Thesis of Prime Mover Engineering Department, Tokai University, March 2014.

14) Y. Izumi, T.Tajikawa, K.Ohba, Y. Uesugi, In vitro experiment on reciprocating flow in a model of the nasal cavities and pharynx, *The Proceedings of the 19th Bioengineering Conference*, *The Japan Society of Mechanical Engineers,* 2007.

15) J. H. Lee, Y. Na, S. K. Kim, S. K. Chung, Unsteady flow characteristics through a human nasal airfway. *Respiratory Physiology and Neurobilogy*, 172, 136-146, 2010.

16) S. Yu, Y. Liu, X. Sun, S. Li, Influence of nasal structure on the distribution of airflow in nasal cavity, *Rhinology*, 46, 137-143, 2008.

17) J. H. Lee, Y. Na, S. K. Kim, S. K. Chung, Unsteady flow characteristics through a human nasal airway, *Respiratory Physiology and Neurobiology*, 172, 136-146, 2010.

18) C.E. Rennie, C.M. Hood, E.J.S.M. Blenke, R.S. Schroter, D.J. Doory, et al., Physical and Computational Modeling of Ventilation of the Maxillary Sinus, *Head and Neck Surgery*, pp.164-170, 2011.

19) Jon o. Lundberg, Nitric oxide and the Paranasal sinus, *The anatomical record*, 291, 1479-1484, 2008.

20) J. H. Zhu, K. M. Lim, K. T. M. Thong, Assessment of airflow ventilation in human nasal cavity and maxillary sinus before and after targeted sinonasal surgery: A numerical case study, *Respiratory Physiology and Neurobiology*, 194, 29-36, 2014.